

# Learning Model Predictive Control with Error Dynamics Regression for Autonomous Racing

Haoru Xue<sup>1</sup>, Edward L. Zhu<sup>2</sup>, and Francesco Borrelli<sup>2</sup>

**Abstract**—This work presents a novel Learning Model Predictive Control (LMPC) strategy for autonomous racing at the handling limit that can iteratively explore and learn unknown dynamics in high-speed operational domains. We start from existing LMPC formulations and modify the system dynamics learning method. In particular, our approach uses a nominal, global, nonlinear, physics-based model with a local, linear, data-driven learning of the error dynamics. We conduct experiments in simulation, 1/10th scale hardware, and deployed the proposed LMPC on a full-scale autonomous race car used in the Indy Autonomous Challenge (IAC) with closed loop experiments at the Putnam Park Road Course in Indiana, USA. The results show that the proposed control policy exhibits improved robustness to parameter tuning and data scarcity. Incremental and safety-aware exploration toward the limit of handling and iterative learning of the vehicle dynamics in high-speed domains is observed both in simulations and experiments.

## I. INTRODUCTION

Recent progress in autonomous racing research has empowered full-size autonomous race cars at or near the top speed of a professional human racing series. Algorithms that were previously experimented with on small-scale vehicles [1] are deployed and further researched on professional race car platforms. Specifically, the teams in the Indy Autonomous Challenge (IAC) [2], starting in 2021, have been demonstrating multi-agent competition above 240 km/h [3].

In the field of control, which is tasked with trajectory tracking at the limit of vehicle dynamics handling, various Model Predictive Control (MPC) techniques remain the state-of-the-art on full-size race car systems. These variations of MPC algorithms solve a finite-horizon optimal control problem (FHOCPP) by computing optimal actuation commands for a vehicle modeled with kinematic or dynamic models, subject to certain track boundary and state constraints [4], [5], [6], [7]. However, for high-speed racing, the performance of classic, nonadaptive MPC methods is ultimately bounded by the fidelity of the vehicle dynamics model. Inaccurate vehicle models will not only induce suboptimal behavior such as weaving, hunting, and steady-state tracking error, but also become dangerous at the handling limit, especially when the model overpredicts this limit. This introduces a chicken-and-egg problem for autonomous racing research at the handling limit: to safely achieve higher speed levels requires more vehicle dynamics data; but to acquire high-speed data requires the controller to achieve higher speed

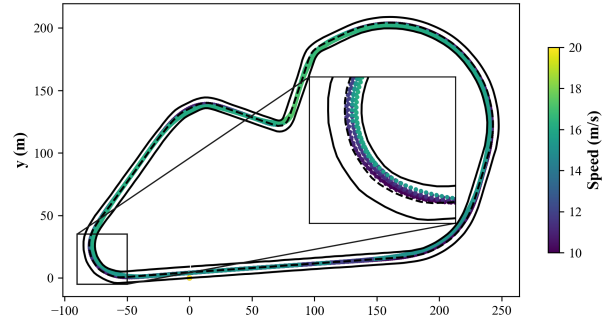


Fig. 1: Overlay of the IAC car’s trajectory running LMPC with error dynamics regression. The data is collected at the Putnam Park Road Course in Indiana, USA. The zoomed-in image of the hairpin turn shows iterative improvement towards optimal cornering.

levels in the first place. Therefore, the motivation of this work is to break the circular problem mentioned earlier by performing incremental and safety-aware exploration toward the limit of handling and iterative learning of the vehicle dynamics in high-speed domains.

In this work, we present a modification to the LMPC approach presented in [8] where we improve significantly upon the model learning strategy. In particular, we propose to learn the error dynamics between a given nominal model and the state evolution of the true system collected during run-time. This is in contrast with the prior approach which attempts to learn a model of the true system directly. We show through simulation and hardware experiments on a 1/10th scale vehicle that our approach exhibits improved robustness to parameter tuning and reduced modeling errors in scenarios when data is scarce for model learning. We finally demonstrate the effectiveness of our approach on a full-size IAC autonomous race car, the results of which are shown in Figure 1. An open source C++ implementation of our work has been made available at <https://github.com/MPC-Berkeley/Racing-LMPC-ROS2>.

*Related Work:* Learning unknown or changing system dynamics has been studied within some classic control frameworks such as adaptive control [9], [10]. System identification is usually part of the controller design, which reasons about some modeling error or noise in the system and adapts the system model to account for them. In autonomous racing, previous works have proposed dynamics learning strategies using Gaussian Processes [11], [12], [13] or implicitly with Gaussian noise assumption [14]. The method is further extended to model multi-vehicle interactions and solve for the optimal overtaking maneuver [15], [16].

Another branch of works exploit the repetitive nature of

<sup>1</sup>Haoru Xue is with the Robotics Institute, Carnegie Mellon University, Pittsburgh, PA, 15213, USA [haorux@andrew.cmu.edu](mailto:haorux@andrew.cmu.edu)

<sup>2</sup>Edward L. Zhu and Francesco Borrelli are with the Department of Mechanical Engineering, University of California Berkeley, Berkeley, CA 94720, USA {[edward.zhu](mailto:edward.zhu), [fborrelli](mailto:fborrelli)}@berkeley.edu

autonomous racing in a single-vehicle scenario, and improves controller performance without any prior assumption about the distribution of the modeling error or noise. Data-driven methods, such as iterative learning control, can optimize the tracking of a repetitive trajectory given data from previous iterations by solving for control variable corrections [17]. More recently, the learning model predictive control (LMPC) framework has been proposed with a direct regression of local affine dynamics [18], [19], [8]. This combination of LMPC and regressive dynamics learning can iteratively learn the unknown system dynamics and reduce lap-time without an explicit prior reference trajectory or a nominal dynamics model. The approach has also been demonstrated on scaled vehicle hardware platforms in [18].

## II. PROBLEM FORMULATION

In this work, we model the vehicle using the planar dynamic bicycle model [20], [21] with state and input vectors:

$$\begin{aligned} x &= [v_x, v_y, \omega_z, e_\psi, s, e_y]^\top \in \mathbb{R}^6 \\ u &= [a, \delta]^\top \in \mathbb{R}^2 \end{aligned}$$

where  $v_x$ ,  $v_y$ , and  $\omega_z$  are the vehicle's longitudinal velocity, lateral velocity, and yaw rate at the center of gravity.  $s$ ,  $e_y$ , and  $e_\psi$  are the pose of the vehicle expressed in the Frenet frame w.r.t. a parametric path  $\tau : [0, L] \mapsto \mathbb{R}^2$ , which is assumed to be continuously twice differentiable and of total length  $L$ . In particular, when given an arclength  $s \in [0, L]$ ,  $\tau$  returns the global  $x$ - $y$  position of the path. In the case where  $\tau$  forms a closed circuit, i.e.  $\tau(0) = \tau(L)$ ,  $\tau'(0) = \tau'(L)$ ,  $\tau''(0) = \tau''(L)$ , where  $\tau'$  and  $\tau''$  are the element-wise first and second derivatives of  $\tau$ , we define the circuit as  $\bar{\tau}(s) = \tau(\text{mod}(s, L))$  for  $s \geq 0$ , where  $\text{mod}$  is the modulo operator. Given a path  $\tau$  and a vehicle with global position  $p = (x, y)$  and heading  $\psi$ , the Frenet frame pose is defined as the vehicle's path progress  $s(p) = \arg \min_s \|\tau(s) - p\|_2$ , its lateral deviation from the path  $e_y(p) = \min_s \|\tau(s) - p\|_2$ , and its heading deviation from the path tangent  $e_\psi(p, \psi) = \psi - \arctan(\tau'(s(p)))$ . The inputs to the model are the longitudinal acceleration  $a$  and the front steering angle  $\delta$ . We write the discretized nonlinear dynamics as:

$$x_{k+1} = f(x_k, u_k) \quad (1)$$

The vehicle's state and input are subject to the constraints  $\mathcal{X} = \{x \mid -W/2 \leq e_y \leq W/2\}$  and  $\mathcal{U} = \{u \mid u_l \leq u \leq u_u\}$ , which describe the boundary constraints for a track of constant width  $W$  and the limits on achievable acceleration and steering angle.

The objective of this work is to design a control policy which solves the infinite-horizon, minimum lap time, optimal control problem:

$$T = \min_{u_0, u_1, \dots} \sum_{k=0}^{\infty} \mathbb{1}_{\mathcal{F}}(x_k) \quad (2a)$$

$$\text{subject to } x_0 = \bar{x}, \quad (2b)$$

$$x_{k+1} = f(x_k, u_k), \quad (2c)$$

$$x_k \in \mathcal{X}, \quad u_k \in \mathcal{U}, \quad (2d)$$

where  $\bar{x} \in \mathcal{S} = \{x \mid s = 0\}$  is a state at the start of the track and  $\mathcal{F} = \{x \mid s \geq L\}$  is the set of states beyond the finish line of the circuit. If for some time step  $k$ ,  $x_k \in \mathcal{F}$  for the first time, then the vehicle has finished the lap and has transitioned onto the next lap.  $\mathbb{1}_{\mathcal{F}}$  is the indicator function for the set  $\mathcal{F}$ , which is defined as

$$\mathbb{1}_{\mathcal{F}}(x) = \begin{cases} 0 & \text{if } x \in \mathcal{F} \\ 1 & \text{o.w.} \end{cases}$$

Due to the infinite horizon cost in (2a), it should be clear that the optimal control problem posed in (2) is not amenable to online implementation. Moreover, it is likely that there is mismatch between the vehicle model in (2c) and the true vehicle dynamics, the effects of which would be especially apparent at high speeds where the vehicle is operating at the limit of handling. To address these challenges, previous work on LMPC [19], [22] proposed a finite-horizon convex approximation of (2), which uses state and input trajectories from prior laps to synthesize a convex terminal cost-to-go function and target set. The same data is additionally used to identify affine time-varying (ATV) models which approximate the true dynamics of the vehicle. In this work, we carry over the same approach for terminal cost-to-go function and target set synthesis, but propose a modification to the system identification procedure which results in an LMPC control policy that achieves similar performance to [19], [22] w.r.t. minimum lap time, while exhibiting a significant improvement in robustness to tuning parameters.

## III. LOCAL LEARNING MODEL PREDICTIVE CONTROL

In this section, we briefly describe the procedure for synthesizing LMPC policies over iterations (or laps) of the minimum time control task. For further details, we refer the reader to [19], [22].

The main idea of LMPC is to use the data from iterations 1 to  $j - 1$  to synthesize a finite-horizon local convex approximation of (2) for iteration  $j$ , which is then solved in a receding horizon manner. Let us first denote the available dataset at iteration  $j$  as  $\mathcal{D}^j = (\mathbf{x}^j, \mathbf{u}^j) \cup \mathcal{D}^{j-1}$ , where  $\mathbf{x}^j = \{x_0^j, x_1^j, \dots, x_{T^j}^j\}$  and  $\mathbf{u}^j = \{u_0^j, u_1^j, \dots, u_{T^j}^j\}$  are the closed-loop state and input sequence for iteration  $j$  and  $T^j$  denotes the time step at which the lap was completed for iteration  $j$ , i.e. the first time step where  $\mathbb{1}_{\mathcal{F}}(x_k) = 0$ . Note that on the first iteration, the dataset  $\mathcal{D}^0$  may be initialized using human-driven laps or closed-loop trajectories from a simple low-speed center-line tracking controller. In addition, we assume that the trajectories stored in  $\mathcal{D}^j$  are feasible w.r.t. the constraints (2d) and reach the finish line in a finite amount of time.

### A. Local Convex Target Set

As the closed-loop trajectories stored in  $\mathcal{D}^j$  are from the actual vehicle, it is straightforward to see that if we can control the vehicle to any state in  $\mathcal{D}^j$ , then there exists a known feasible control sequence which can be used to complete the lap from that state. LMPC uses this fact to construct a safe set as a discrete collection of the states in  $\mathcal{D}^j$ , which is then used as the terminal set for a FHOCP [22].

In this work, we construct convex terminal sets which are local about a given state  $x$ . These terminal sets sacrifice the theoretical guarantee of persistent feasibility for the FHOCP in favor of reduced computational complexity for fast online control. In particular, for some given state  $x$ , we first take the  $K$ -nearest neighbors from the each of the previous  $P$  laps by evaluating the weighted Euclidean distance over the relevant states:

$$(x_k^i - x)^\top D(x_k^i - x), \forall i \in \{j, j-1, \dots, j-(P-1)\}, \\ k \in \{0, 1, \dots, T^i\} \quad (3)$$

for some given  $P$  and  $D \succeq 0$ . Let  $\mathbf{X}^j(x; \mathcal{D}^j) \in \mathbb{R}^{n \times KP}$  denote the matrix formed by the  $KP$  states closest to  $x$ , we then define the target set as the convex hull of these states:

$$\mathcal{X}_N^j(x; \mathcal{D}^j) = \{\bar{x} \in \mathbb{R}^n \mid \exists \lambda \in \mathbb{R}^{KP}, 0 \leq \lambda \leq 1, \mathbf{1}^\top \lambda = 1, \\ \mathbf{X}^j(x; \mathcal{D}^j) \lambda = \bar{x}\}$$

### B. Local Terminal Cost-to-go Function

By assumption, the closed-loop state trajectories stored in  $\mathcal{D}^j$  reach the finish line in a finite amount of time. We can therefore compute the cost-to-go for any state  $x_k^i$  in  $\mathcal{D}^j$  as  $T^i - k$ , which represents the time remaining to finish the  $i$ -th lap for  $i \in \{0, \dots, j\}$ . Let  $J_N^j(x; \mathcal{D}^j) \in \mathbb{R}^{KP}$  denote the vector of cost-to-go values calculated for the states in  $\mathbf{X}^j(x; \mathcal{D}^j)$ . We can therefore define the minimum cost-to-go function for any  $\bar{x} \in \mathcal{X}_N^j(x; \mathcal{D}^j)$  as:

$$Q_N^j(\bar{x}, x; \mathcal{D}^j) \\ = \min_{\lambda \in \mathbb{R}^{KP}} J_N^j(x; \mathcal{D}^j)^\top \lambda \\ \text{subject to } 0 \leq \lambda \leq 1, \mathbf{1}^\top \lambda = 1, \mathbf{X}^j(x; \mathcal{D}^j) \lambda = \bar{x}$$

This function can be thought of as a local convex approximation to the optimal cost-to-go (from solving (2)) at iteration  $j$ , which when incorporated as the terminal cost-to-go function, allows an FHOCP to reason about infinite-horizon behavior of the vehicle, to the extent as it is captured in the dataset.

### C. Local LMPC

Using the terminal target set and cost-to-go function synthesized from the dataset  $\mathcal{D}^{j-1}$ , we may now construct the FHOCP at time step  $k$  of iteration  $j$  for our local LMPC policy as follows:

$$J_k^j(x_k, u_{k-1}, \bar{\mathbf{z}}_k; \mathcal{D}^{j-1}) = \\ \min_{\mathbf{x}, \mathbf{u}, \lambda} \sum_{t=0}^{N-1} \mathbb{1}_{\mathcal{F}}(x_t) + c_u \|u_t\|_2^2 + c_{\Delta u} \|u_t - u_{t-1}\|_2^2 \\ + J_N^{j-1}(\bar{x}_{k+N}; \mathcal{D}^{j-1})^\top \lambda \quad (4a)$$

$$\text{subject to } x_0 = x_k, u_{-1} = u_{k-1} \quad (4b)$$

$$x_{t+1} = A(\bar{z}_{k+t}; \mathcal{D}^{j-1})x_t + B(\bar{z}_{k+t}; \mathcal{D}^{j-1})u_t \\ + C(\bar{z}_{k+t}; \mathcal{D}^{j-1}), t \in \{0, \dots, N-1\}, \quad (4c)$$

$$x_t \in \mathcal{X}, u_t \in \mathcal{U}, t \in \{0, \dots, N\} \quad (4d)$$

$$\mathbf{X}^{j-1}(\bar{x}_{k+N}; \mathcal{D}^{j-1}) \lambda = x_N, \quad (4e)$$

$$0 \leq \lambda \leq 1, \mathbf{1}^\top \lambda = 1 \quad (4f)$$

where  $\bar{z}_k = (\bar{x}_k, \bar{u}_k)$  and  $\bar{\mathbf{z}}_k = \{\bar{z}_k, \dots, \bar{z}_{k+N}\}$  is a state and input sequence which is used to form the local convex approximation. In practice, this is chosen as the solution to (4) from the previous time-step. Construction of the  $A$ ,  $B$ , and  $C$  matrices in the ATV dynamics (4c) is the main contribution of this work and will be discussed in the next section. Note that (4) is a convex program which can be solved efficiently using existing solvers.

Finally, let  $\mathbf{u}^* = \{u_0^*, \dots, u_{N-1}^*\}$  be the optimal control sequence which solves (4) at time step  $k$ . The input  $u_k = u_0^*$  is applied to the vehicle and the FHOCP (4) is repeated at time step  $k+1$  for the measured state  $x_{k+1}$  until the vehicle reaches the finish line, at which point  $\mathcal{D}^j$  will be constructed using the closed-loop trajectory for lap  $j$ .

## IV. LEARNED VEHICLE DYNAMICS MODEL

We now introduce the main contribution of our work, which is a learning strategy on the dynamics states  $v_x, v_y, \omega_z$  based on regressive error. The learning process take as inputs the nominal dynamics model and a set of neighboring states, and outputs a learned local affine approximation of the true vehicle dynamics.

We assume that the true dynamics of the system can be written as follows

$$x^+ = f(x, u) + e(x, u), \quad (5)$$

where  $f$  are the nominal dynamics from (1) and  $e$  denotes some unknown modeling error which we would like to identify using data. For a given state and input  $x$  and  $u$ , let us denote the prediction of the nominal model as  $\hat{x}^+ = f(x, u)$ . We may now linearize the error dynamics about a reference state and input  $\bar{z}$  as follows:

$$x^+ - \hat{x}^+ = A^e x + B^e u + C^e, \quad (6)$$

where  $A^e$  and  $B^e$  are the Jacobians of  $e$  w.r.t.  $x$  and  $u$  evaluated at  $\bar{z}$  and  $C^e = e(\bar{x}, \bar{u}) - A^e \bar{x} - B^e \bar{u}$ . It can be clearly seen from (6) that the linearization of the unknown error term is related to the system state and input  $x$  and  $u$ , the actual state evolution  $x^+$ , and the prediction of the nominal model  $\hat{x}^+$ , which are all quantities that can be easily obtained from the dataset  $\mathcal{D}^{j-1}$  at iteration  $j$ . As such, we query  $\mathcal{D}^{j-1}$  to find the  $M$  nearest neighbors  $\mathbf{z} = \{z_1, \dots, z_M\}$  of  $\bar{z}$  and their corresponding state evolutions  $\mathbf{x}^+ = \{x_1^+, \dots, x_M^+\}$  (using a technique similar to (3)). We then compute the prediction of nominal model at each of the state and input pairs in  $\mathbf{z}$  to obtain  $\hat{\mathbf{x}}^+ = \{\hat{x}_1^+, \dots, \hat{x}_M^+\}$ . As mentioned before, we are interested in learning only the error dynamics associated with the velocity components of the state  $x$  as the kinematic components of the state are well-understood. Therefore, using the datasets  $\mathbf{z}$ ,  $\mathbf{x}^+$ , and  $\hat{\mathbf{x}}^+$ , we define the residuals for each velocity state as follows:

$$A^e[11 : 13]x_m[1 : 3] + B^e[11]a_m + C^e[1] = v_{x,m}^+ - \hat{v}_{x,m}^+, \\ A^e[21 : 23]x_m[1 : 3] + B^e[22]\delta_m + C^e[2] = v_{y,m}^+ - \hat{v}_{y,m}^+, \\ A^e[31 : 33]x_m[1 : 3] + B^e[32]\delta_m + C^e[3] = \omega_{z,m}^+ - \hat{\omega}_{z,m}^+, \quad (7)$$

where  $m \in \{1, \dots, M\}$  and we use the notation  $A[11 : 13]$  to index the first three elements of the first row of matrix

A. Note that we have injected additional structure into the individual residuals by making explicit the dependence of each velocity state on a certain subset of the input components. From these three expressions, we define the following regressor vectors:

$$\Gamma_{v_x} = \begin{bmatrix} A^e[11:13] \\ B^e[11] \\ C^e[1] \end{bmatrix}, \Gamma_{v_y} = \begin{bmatrix} A^e[21:23] \\ B^e[22] \\ C^e[2] \end{bmatrix}, \Gamma_{\omega_z} = \begin{bmatrix} A^e[31:33] \\ B^e[32] \\ C^e[3] \end{bmatrix}.$$

We solve the regression problem in a manner similar to [8], where we weigh the importance of data point  $m$  using the Epanechnikov kernel function [23] with bandwidth  $h$ :

$$K(u) = \begin{cases} \frac{3}{4}(1 - u^2/h^2), & |u| < h \\ 0, & \text{otherwise} \end{cases}.$$

such that larger penalties are assigned to the residuals for data points that are close to the linearization point  $\bar{x}$ . For  $l = \{v_x, v_y, \omega_z\}$ , the weighted least squares problem is defined as follows:

$$\Gamma_l^* = \operatorname{argmin}_{\Gamma_l} \sum_{m=1}^M K(\|\bar{x} - x_m\|_Q^2) y_m^l(\Gamma_l),$$

where  $Q$  denotes the relative scaling between the variables, and  $y_m^l(\Gamma_l)$  are the  $l^2$ -norms of the residuals in (7).

Finally, we can unpack the optimal regressor vectors  $\Gamma_l^*$  to construct the matrices  $A^e$ ,  $B^e$ , and  $C^e$ , and add them to the nominal ATV dynamics to obtain the complete ATV model for (4c):

$$A(\bar{z}; \mathcal{D}^{j-1}) = A^f + \begin{bmatrix} \Gamma_{v_x}^*[1:3] & & \\ \Gamma_{v_y}^*[1:3] & & \\ \Gamma_{\omega_z}^*[1:3] & & \\ \mathbf{0}_{3 \times 3} & & \mathbf{0}_{6 \times 3} \end{bmatrix},$$

$$B(\bar{z}; \mathcal{D}^{j-1}) = B^f + \begin{bmatrix} \Gamma_{v_x}^*[4] & 0 \\ 0 & \Gamma_{v_y}^*[4] \\ 0 & \Gamma_{\omega_z}^*[4] \\ \mathbf{0}_{3 \times 2} & \end{bmatrix},$$

$$C(\bar{z}; \mathcal{D}^{j-1}) = C^f + [\Gamma_{v_x}^*[5] \quad \Gamma_{v_y}^*[5] \quad \Gamma_{\omega_z}^*[5] \quad \mathbf{0}_{1 \times 3}]^\top,$$

where  $A^f$  and  $B^f$  are the Jacobians of  $f$  w.r.t.  $x$  and  $u$  evaluated at  $\bar{z}$  and  $C^f = f(\bar{x}, \bar{u}) - A^f \bar{x} - B^f \bar{u}$ . We note that the key difference of this procedure compared to [8] is that the regressive learning is performed on the *error* between the prediction of the nominal model and the actual state evolution data instead of on the entire model in (5) all at once. This strategy not only provides a safety fallback when the regressive learning fails at run-time, but also demonstrates, in comparison to [8], improved robustness to parameter tuning and reduced modeling errors in scenarios when data is scarce.

## V. EXPERIMENTS & RESULTS

We now present a set of experiments in simulation and hardware to demonstrate the effectiveness of combining LMPC and error dynamics regression in autonomous racing. The key metrics throughout these experiments are

- 20th iteration lap time (ILT-20): the average lap time after running the LMPC for 20 iterations. The shorter

the lap time, the better the performance of the control policy.

- Iteration to fail (ITF): the average number of iterations before an experiment fails due to loss of control or track boundary violation. We set the maximum number of iterations in an experiment to 20 laps around the track.

### A. Robustness Study on Learning Parameters

This experiment aims to study how LMPC parameter tunings affect the safety of the learning process. The motivation is that there are not many trial-and-error opportunities when tuning parameters on safety-critical hardware such as a race car, and a robust control setup should be able to handle a broad range of parameter settings without destabilizing the system. We set up simulation experiments to compare our approach against the LMPC implementation in [8] in terms of their robustness to the change in the control-rate cost (CRC) ( $c_{\Delta u}$  in (4a)). Intuitively the CRC is analogous to the ‘‘learning rate’’ for LMPC. A higher CRC will penalize drastic changes in the control input and keep the vehicle closer to the safe set over the MPC horizon. It is therefore a key parameter when tuning the behavior of the LMPC policy.

In simulation, we ran both LMPC implementations with 5 different CRCs across two orders of magnitude and recorded the lap time and average velocity at every iteration. The simulation model is formulated to be as close as possible to the 1/10th scale vehicle used in the following hardware experiment. For fairness of comparison, we purposely introduced a mismatch in the tire-road friction coefficient  $\mu$  in our nominal dynamics model. Whereas a value of 0.9 is used in the simulation model, a value of 1.2 is chosen for the LMPC nominal dynamics model in (1), which is typically only seen on full scale race cars with racing slick tires. This would have induced dangerous over-confidence in the model about the surface friction, as shown in the following hardware experiments, if no dynamics learning is used.

Table I presents the key results of this experiment. We swept CRC from 1.0 to 0.01 and compared the performance of the two LMPC implementations. With a high CRC penalty (experiments 1 and 2), both [8] and ours fail to reach the optimal lap time in 20 iterations, with [8] achieving a more significant lap time reduction. However, once we decrease the CRC to 0.1, [8] starts to fail at around lap 8, whereas our method exhibits greater robustness to different settings of the CRC and can converge to the optimal lap time within 20 iterations once the CRC drops below 0.1. Figure 3 compares the per-iteration performance of both methods, showing that [8] fails with more than half of the CRC settings, while our approach was able to keep the system safe for all settings.

To understand how the accuracy of the learned model compares between the two approaches, we inspect the average norm of the difference between the learned dynamics matrix  $A(\bar{z}, \mathcal{D}^{j-1})$  and the actual local dynamics matrix of the simulation model, which is computed by taking the Jacobian of the true system model at the same points  $\bar{z}$ . Figure 2 shows the evolution of the mismatch in the dynamics matrix over laps of a simulation experiment with a CRC value of 1. We

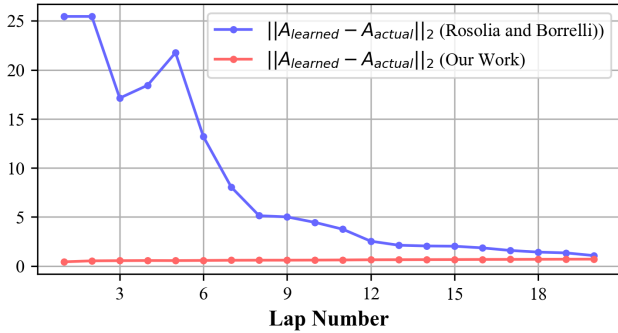


Fig. 2: Comparison of average learned model error per iteration for a simulation experiment.

Experiment #	Control Rate Cost	ILT-20		ITF	
		[8]	ours	[8]	ours
1	1.0	<b>8.5</b>	11.8	20+	20+
2	0.5	<b>6.6</b>	9.5	20+	20+
3	0.1	-	<b>6</b>	9	<b>20+</b>
4	0.05	-	<b>4.9</b>	8	<b>20+</b>
5	0.01	-	<b>4.8</b>	4	<b>20+</b>

TABLE I: Results of the robustness study. An ITF of 20+ means that the algorithm did not fail in the 20-iteration experiment.

highlight that although the modeling error of full dynamics regression in [8] eventually reaches the same level as our error dynamics regression, our learning approach better approximates the actual local dynamics consistently and always only shows a small model mismatch after learning. This is especially important in the initial iterations when there is relatively scarce data to accurately fit an ATV model. We believe that this large initial model mismatch with [8] may have contributed to the failure cases with lower settings of CRC, as the LMPC is unintentionally reaching the handling limit due to exploiting a poorly fitted model before sufficient data can be collected to perform an accurate regression of the full dynamics.

Overall, our simulation experiments suggest that LMPC with error dynamics regression exhibits greater stability and robustness to key parameter settings and works well even when scarce dynamics data is available. These properties could potentially make the system more suitable for hardware deployment in safety-critical applications.

### B. Hardware Experiment Comparing Learning Performance

In this section, we present results from physical experiments with the Berkeley Autonomous Race Car (BARC) platform. These robotic vehicles are based on 1/10 scale, off-the-shelf RC cars that have been heavily modified to support autonomous vehicle architecture. Their specifications are listed in Table II. LMPC computation is done off-board on a laptop computer and localization is provided by a motion capture system.

In total, we conducted four sets of experiments. In the first two sets, the LMPC proposed in [8] is run on the BARC platform without any regressive learning of the vehicle dynamics. In the first case, we purposefully under-estimate the vehicle handling limit by reducing the tire-road friction coefficient to  $\mu = 0.7$  in the nominal model. In the second case, we over-estimate by setting the coefficient to  $\mu = 1.2$ . Note that the actual tire-road friction coefficient was measured to be

Specification	BARC	IAC Car
Mass	2.2 kg	800 kg
Wheelbase	0.26 m	4 m
Top Speed	$\sim 10$ km/h	$\sim 320$ km/h
Top Lateral Acceleration	$\sim 10$ -15 $m/s^2$	$\sim 15$ -20 $m/s^2$
Top Longitudinal Acceleration	$\sim 10$ -15 $m/s^2$	$\sim 10$ -15 $m/s^2$
Top Braking	$\sim 10$ -15 $m/s^2$	$\sim 20$ -30 $m/s^2$
Max Engine Power	$\sim 100$ W	$\sim 340$ kW

TABLE II: Vehicle specifications of BARC and IAC platforms used in this work.

LMPC Configuration	Avg. ILT-20	Avg. ITF
No regression ( $\mu = 0.7$ )	6.292	<b>20+</b>
No regression ( $\mu = 1.2$ )	<b>5.42</b>	18.9
Full Dynamics Regression ([8])	-	4.2
Error Dynamics Regression (Ours)	5.51	<b>20+</b>

TABLE III: Key metrics of the BARC hardware experiment. A hyphen in the ILT-20 column means that the algorithm fails before the 20th iteration. An ITF of 20+ means that the algorithm did not fail over the 20 laps.

0.9. The last two sets of experiments are done with the full dynamics learning from [8] and our error dynamics learning strategy, respectively. Each set of experiments consists of 10 runs under constant LMPC tuning with  $CRC = 0.1$ , each lasting at most 20 iterations. We record the lap times and record any failure cases before the 20-iteration threshold.

Table III compares the metrics in these four sets of experiments. When the LMPC is run with  $\mu = 0.7$ , the car is no longer able to reach the optimal lap time, presumably because the mismatched dynamics lead the controller to under-estimate the handling limit. With  $\mu = 1.2$ , although the LMPC is still able to achieve the same lap time as our work, it fails during several trials after 17-19 iterations due to track constraint violation, exhibiting borderline unsafe behaviors. We next compare the two regressive learning strategies. Under this low CRC setting, LMPC with full dynamics regression [8] attempts to improve the lap time quickly, but eventually fails after no more than 5 iterations in all 10 trials. On the other hand, our method converges to a best lap time safely in all experiments, while exhibiting faster lap time reduction when compared to the cases of no dynamics learning, as shown in Figure 4. We note that although Figure 4 seems to suggest that simply over-estimating the vehicle handling limit could also lead to optimal lap times, it comes at the cost of a lower ITF value and is potentially more dangerous. Figure 5 visualizes the vehicle’s trajectory over iterations with our regressive learning strategy, which shows convergence towards an optimal race line.

### C. Hardware Demonstration on a Full-Size Race Car

In this demonstration, we deployed our LMPC and error dynamics regression strategy on a full-size *IndyLights* race car which has been used in the Indy Autonomous Challenge [3]. The key specifications of the vehicle are listed in Table II. The race track used for this demonstration is the Putnam Park Road Course in Indiana, USA. We construct the initial dataset  $\mathcal{D}^0$  for the vehicle by running a tracking MPC on the center line of the track at 10 m/s for 3 laps. We note that this step could also be done with a more rudimentary controller. We then ran LMPC with error dynamics regression for 10

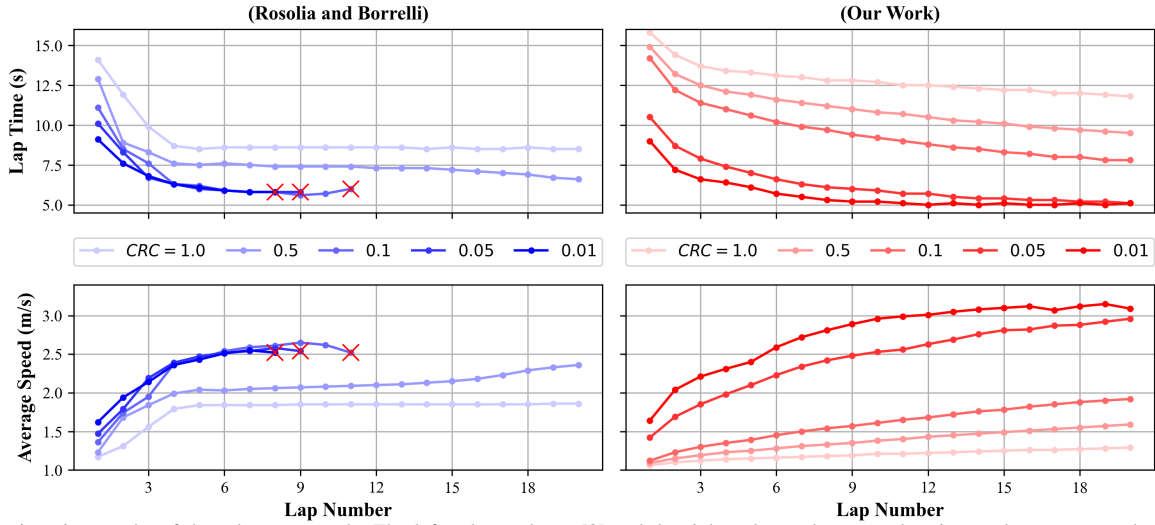


Fig. 3: Per-iteration results of the robustness study. The left column shows [8] and the right column shows our lap time and average speed with different control-rate cost (CRC) tunings. A red cross is placed where failure occurs due to unsafe handling of the vehicle by the LMPC.

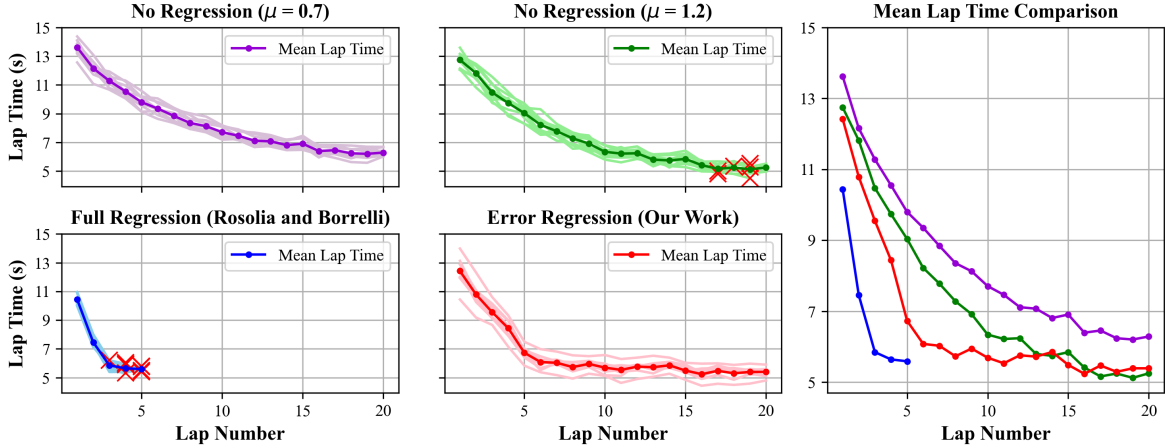


Fig. 4: Per-iteration results of the BARC hardware experiment. The four smaller plots on the left show the lap-time reduction of the 10 trials. The combined plot on the right compares the average lap time achieved. A red cross is placed where failure occurs due to unsafe handling of the vehicle by the LMPC.

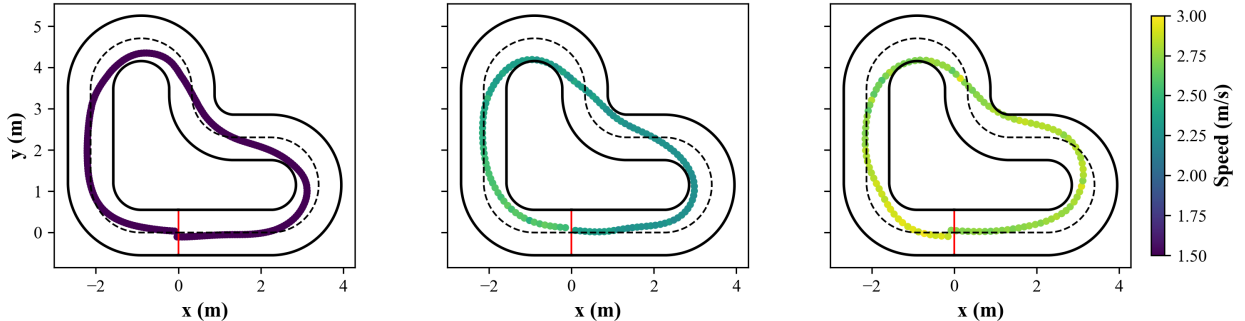


Fig. 5: Visualization of the 1st, 5th and 20th iteration's trajectory of LMPC with error dynamics regression on the BARC platform.

iterations. Figure 1 visualizes the trajectory driven by the vehicle, with a zoomed-in view to highlight how LMPC optimizes the shape of the trajectory for a hairpin turn. It can be clearly seen in Figure 1 that the vehicle starts at lower speeds closer to the center line and incrementally increases its speed through the corners and approaches the track boundary constraint.

## VI. CONCLUSION

This work proposes a new error dynamics learning approach under the LMPC framework to iteratively and safely

explore the boundary of vehicle handling limit in autonomous racing. We based the learning on a nominal dynamics model, which provides explainability and safety fallback for the learning process. We then derived the regression method on top to learn a local approximation of the nonlinear model mismatch. Through simulation and hardware experiments, we showed that our method exhibits greater robustness against parameter tuning and data scarcity compared with previous LMPC works, and offers new potential solutions to address the challenge of vehicle dynamics data acquisition in high-speed autonomous racing.

## REFERENCES

- [1] M. O’Kelly, H. Zheng, D. Karthik, and R. Mangharam, “FITENTH: An Open-source Evaluation Environment for Continuous Control and Reinforcement Learning,” in *Proceedings of the NeurIPS 2019 Competition and Demonstration Track*. PMLR, Aug. 2020, pp. 77–89.
- [2] “Indy Autonomous Challenge,” Feb. 2023. [Online]. Available: <https://www.indyautonomouschallenge.com>
- [3] A. Wischnewski, M. Geisslinger, J. Betz, T. Betz, F. Fent, A. Heilmeyer, L. Hermansdorfer, T. Herrmann, S. Huch, P. Karle, F. Nobis, L. Ögretmen, M. Rowold, F. Sauerbeck, T. Stahl, R. Trauth, M. Lienkamp, and B. Lohmann, “Indy autonomous challenge – autonomous race cars at the handling limits,” 2022.
- [4] A. Wischnewski, T. Herrmann, F. Werner, and B. Lohmann, “A Tube-MPC Approach to Autonomous Multi-Vehicle Racing on High-Speed Ovals,” *IEEE Transactions on Intelligent Vehicles*, vol. 8, no. 1, pp. 368–378, Jan. 2023.
- [5] J. Kabzan, M. I. Valls, V. J. F. Reijgwart, H. F. C. Hendrikx, C. Ehmke, M. Prajapat, A. Bühler, N. Gosala, M. Gupta, R. Sivanesan, A. Dhall, E. Chisari, N. Karnchanachari, S. Brits, M. Dangel, I. Sa, R. Dubé, A. Gawel, M. Pfeiffer, A. Liniger, J. Lygeros, and R. Siegwart, “AMZ Driverless: The full autonomous racing system,” *Journal of Field Robotics*, vol. 37, no. 7, pp. 1267–1294, 2020.
- [6] J. Betz, T. Betz, F. Fent, M. Geisslinger, A. Heilmeyer, L. Hermansdorfer, T. Herrmann, S. Huch, P. Karle, M. Lienkamp, B. Lohmann, F. Nobis, L. Ögretmen, M. Rowold, F. Sauerbeck, T. Stahl, R. Trauth, F. Werner, and A. Wischnewski, “TUM autonomous motorsport: An autonomous racing software for the Indy Autonomous Challenge,” *Journal of Field Robotics*, vol. 40, no. 4, pp. 783–809, 2023.
- [7] J. Funke, P. Theodosis, R. Hindiyeh, G. Stanek, K. Kritatakirana, C. Gerdes, D. Langer, M. Hernandez, B. Müller-Bessler, and B. Huhnke, “Up to the limits: Autonomous Audi TTS,” in *2012 IEEE Intelligent Vehicles Symposium*, Jun. 2012, pp. 541–547.
- [8] U. Rosolia and F. Borrelli, “Learning How to Autonomously Race a Car: A Predictive Control Approach,” *IEEE Transactions on Control Systems Technology*, vol. 28, no. 6, pp. 2713–2719, Nov. 2020.
- [9] M. Bujarbaruah, X. Zhang, U. Rosolia, and F. Borrelli, “Adaptive mpc for iterative tasks,” in *2018 IEEE Conference on Decision and Control (CDC)*. IEEE, 2018, pp. 6322–6327.
- [10] A. Sasfi, M. N. Zeilinger, and J. Köhler, “Robust adaptive mpc using control contraction metrics,” *Automatica*, vol. 155, p. 111169, 2023.
- [11] J. Kabzan, L. Hewing, A. Liniger, and M. N. Zeilinger, “Learning-based model predictive control for autonomous racing,” *IEEE Robotics and Automation Letters*, vol. 4, no. 4, pp. 3363–3370, 2019.
- [12] L. Hewing, A. Liniger, and M. N. Zeilinger, “Cautious NMPC with Gaussian Process Dynamics for Autonomous Miniature Race Cars,” in *2018 European Control Conference (ECC)*, Jun. 2018, pp. 1341–1348.
- [13] J. Ning and M. Behl, “Vehicle dynamics modeling for autonomous racing using gaussian processes,” 2023.
- [14] D. Kalaria, Q. Lin, and J. M. Dolan, “Delay-aware robust control for safe autonomous driving,” in *2022 IEEE Intelligent Vehicles Symposium (IV)*, 2022, pp. 1565–1571.
- [15] E. L. Zhu, F. L. Busch, J. Johnson, and F. Borrelli, “A gaussian process model for opponent prediction in autonomous racing,” 2023.
- [16] T. Brüdigam, A. Capone, S. Hirche, D. Wollherr, and M. Leibold, “Gaussian process-based stochastic model predictive control for overtaking in autonomous racing,” 2021.
- [17] D. Bristow, M. Tharayil, and A. Alleyne, “A survey of iterative learning control,” *IEEE Control Systems Magazine*, vol. 26, no. 3, pp. 96–114, 2006.
- [18] U. Rosolia and F. Borrelli, “Learning Model Predictive Control for Iterative Tasks: A Computationally Efficient Approach for Linear System,” *IFAC-PapersOnLine*, vol. 50, no. 1, pp. 3142–3147, Jul. 2017.
- [19] M. Brunner, U. Rosolia, J. Gonzales, and F. Borrelli, “Repetitive learning model predictive control: An autonomous racing example,” in *2017 IEEE 56th annual conference on decision and control (CDC)*. IEEE, 2017, pp. 2545–2550.
- [20] J. Kong, M. Pfeiffer, G. Schildbach, and F. Borrelli, “Kinematic and dynamic vehicle models for autonomous driving control design,” *IEEE Intelligent Vehicles Symposium, Proceedings*, vol. 2015-August, pp. 1094–1099, 2015.
- [21] F. Christ, A. Wischnewski, A. Heilmeyer, and B. Lohmann, “Time-optimal trajectory planning for a race car considering variable tyre-road friction coefficients,” *Vehicle System Dynamics*, vol. 59, no. 4, pp. 588–612, Apr. 2021.
- [22] U. Rosolia and F. Borrelli, “Learning model predictive control for iterative tasks. a data-driven control framework,” *IEEE Transactions on Automatic Control*, vol. 63, no. 7, pp. 1883–1896, 2017.
- [23] V. A. Epanechnikov, “Non-Parametric Estimation of a Multivariate Probability Density,” *Theory of Probability & Its Applications*, vol. 14, no. 1, pp. 153–158, Jan. 1969.